ELSEVIER

Chemical Physics 272 (2001) 61–68

Chemical Physics

www.elsevier.com/locate/chemphys

Cl + HD reaction dynamics from quasiclassical trajectory calculation on a new ab initio potential energy surface

Changsheng Shen [a], Tao Wu [a], Guanzhi Ju [a,b,*], Wensheng Bian [c]

[a] *Department of Chemistry, State Key Laboratory of Coordination Chemistry, Mesoscopical Solid State Chemistry Institute, Nanjing University, Nanjing 210093, China*

[b] *State Key Laboratory of Crystal Material, Shandong University, Jinan 250100, China*

[c] *Institute of Theoretical Chemistry, Shandong University, Jinan 250100, China*

Received 3 April 2001

Abstract

The reaction cross-sections, the product energy partitioning and angular distribution, and the product internal state distribution for the Cl + HD reaction have been calculated and discussed by quasiclassical trajectory method with symplectic integration on a new three-dimensional ab initio potential energy surface (PES), named as mBW2 PES. It was found that the DCl to HCl branching ratio on the mBW2 PES is larger than that on the G3 PES when the initial conditions are the same. The effectiveness of translational, vibrational, and rotational energies in promoting reaction is also compared for Cl + HD reaction.

1. Introduction

The dynamics of the ClH_2 reactive system has been the subject of many theoretical and experimental studies [1–10]. Persky and co-workers [11–15] performed quasiclassical trajectory (QCT) calculations for the $Cl + H_2$ reaction and isotopic variants on a semiempirical LEPS (London–Eyling–Polanyi–Sato) PES [11], originally called the GSW PES. The reaction cross-section (S_r), thermal rate constants (k_T), isotopic branching ratios and product energy partitioning for the $Cl + HD \rightarrow HCl(DCl) + D(H)$ reaction were calculated [14] over a wide range of collision energies, E_c, with initial HD vibrational state $v = 0$ and rotational states $j = 0$–4. Aoiz and Bañares [16] reported QCT calculations for the Cl + HD ($v = 0, 1$, $j = 0, 1$) reaction on a partly ab initio PES, called G3 PES [8], at 0.2775 and 0.65 eV collision energies. Kandal et al. [17] provided the first experimental data on product internal state and scattering distributions and isotopic branching ratios at a mean collision energy of 0.065 eV for the Cl + HD ($v = 1$, $j = 1, 2$) reaction. The measured DCl + H to HCl + D branching ratio is at variance with the theoretical calculations that predict about three

* Corresponding author. Address: Department of Chemistry, State Key Laboratory of Coordination Chemistry, Mesoscopical Solid State Chemistry Institute, Nanjing University, Nanjing 210093, China. Tel.: +86-25-359-6955; fax: +86-25-331-7761.

E-mail address: gzju@nju.edu.cn (G. Ju).

0301-0104/01/$ - see front matter
PII: S0301-0104(01)00445-1

times larger yield of HCl + D at this collision energy on the G3 PES.

In addition, the HCl + D/DCl + H branching ratios yielded by the recent molecular beam experiment [10] for Cl + HD at low collision energies are in strong disagreement with QM calculations on G3 potential surface. In order to further improve the PES for the Cl + H_2 reaction, a new ab initio PES called BW2 was constructed by Bian and Werner [18]. On the BW2 PES, Manthe et al. [19] and Yang et al. [20,21] carried out quantum dynamics studies of the Cl + H_2 reaction and Cl + D_2 reaction.

In this work we report the results of QCT calculations for the Cl + HD reaction on the new mBW2 PES, a modified version of the BW2 PES. Reaction cross-sections, the product internal state and angular distribution, and the product energy partitioning were calculated and discussed.

The organization of this paper is as follows: Section 2 introduces the mBW2 PES. Computational details are briefly presented in Section 3. The results of the calculation and a discussion of the results are given in Section 4. Finally, a summary is presented in Section 5.

2. Potential energy surface

The BW1 PES [18] was computed using internally contracted multireference configuration interaction (MRCI) wave functions [22] with complete active space self-consistent field reference wave functions [23]. The Davidson correction [24] (+Q) was applied to the final energies in order to account approximately for unlinked cluster effects of higher excitations. The analytical fits were generated from the computed energies at 1200 geometries. The BW1 PES is based on the original MRCI + Q energies without scaling; the BW2 was generated from the scaled energies, similar to what was done in Truhlar's scaled external correlation correction [25], i.e.

$$E_{\text{Scaled}} = F(E_{\text{MRCI+Q}} - E_{\text{CASSCF}}) + E_{\text{CASSCF}}. \tag{1}$$

The scaling factor F is 1.05485 in BW2 surface, excluding the spin–orbit effect.

The mBW2 PES, used in our QCT calculations, is a modified version of BW2, which includes spin–orbit coupling approximately. The value of F is determined so that the dissociation energies of the diatomic molecules are reproduced correctly,

$$F = \frac{D_e(\text{exp}) - D_e(\text{CASSCF})}{D_e(\text{MRCI} + \text{Q}) - D_e(\text{CASSCF})}, \tag{2}$$

where D_e are the calculated and experimental dissociation energies of HCl or H_2. The experimental dissociation energy of HCl has been corrected for the spin–orbit effect.

The analytic form of the PES is given by

$$V_{\text{ABC}} = \sum_i V_i^{(1)} + \sum_n V_n^{(2)}(R_n) + V_{\text{ABC}}^{(3)}(R_{\text{AB}}, R_{\text{BC}}, R_{\text{AC}}), \tag{3}$$

where $V_i^{(1)}$ (i = A, B, C) are the energies of the atoms, $V_n^{(2)}$ (n = AB, BC, AC) are the diatomic potentials of HCl and H_2, and $V_{\text{ABC}}^{(3)}$ is a three-body potential. The diatomic potentials are expressed as

$$V_{\text{AB}} = \frac{C_0\, e^{(-\alpha_{\text{AB}} R_{\text{AB}})}}{R_{\text{AB}}} + \sum_{i=1}^{6} c_i \rho_{\text{AB}}^i \tag{4}$$

with

$$\rho_{\text{AB}} = R_{\text{AB}}\, e^{(-\beta_{\text{AB}} R_{\text{AB}})}. \tag{5}$$

The three-body potential is expressed as a polynomial of order M,

$$V_{\text{ABC}}^{(3)}(R_{\text{AB}}, R_{\text{BC}}, R_{\text{AC}}) = \sum_{i,j,k}^{M} d_{ijk} \rho_{\text{AB}}^i \rho_{\text{BC}}^j \rho_{\text{AC}}^k \tag{6}$$

with the constraints $i + j + k \neq i \neq j \neq k$ and $M \geqslant i + j + k$. For the sake of symmetry, we have $d_{ijk} = d_{kji}$, $\beta_{\text{AB}} = \beta_{\text{AC}}$. The three-body parameters were determined by fitting the difference of the ab initio energies of the ClH2 system and the sum of the one and two energies at the corresponding geometries.

All of the parameters of mBW2 surface can be downloaded from the web [26].

The BW surfaces (BW1, BW2, mBW2) differ qualitatively from G3 surface in the entrance and exit channels. The BW surfaces have long-range van der Waals minima, which are entirely absent in the LEPS-type G3 surface. In the entrance channel, the BW surfaces are least repulsive for per-

Table 1
Comparison of barrier properties for the $Cl + H_2$ reaction

Surface	R_{ClH}[a]	R_{HH}[a]	Θ[b]	E[c]	ω_i[d]	ω_b[e]	ω_s[f]
G3	2.648	1.870	180	7.88	1520i	581	1358
BW1	2.710	1.850	180	8.14	1333i	543	1356
BW2	2.704	1.854	180	7.61	1294i	540	1360
mBW2	2.708	1.850	180	7.88	1317i	542	1358

[a] Bond distance in bohr.
[b] Bond angle in deg.
[c] Barrier height in kcal/mol.
[d] Imaginary frequency in cm^{-1}.
[e] Bending vibration frequency in cm^{-1}.
[f] Symmetric stretching vibration frequency in cm^{-1}.

pendicular (T-shaped) approach of Cl to H_2, while G3 surface is most repulsive for T-shaped structure. The BW surfaces have a well in the exit channel as in the entrance channel. The comparison of the saddle point properties of BW and G3 surfaces are presented in Table 1. It is found that the saddle points of the BW surfaces are located a little earlier in the entrance channel than that of the G3 surface. The barrier height of the mBW2 surface is equal to that of the G3 surface. However, the mBW2 imaginary frequency corresponding to the asymmetric stretch is substantially smaller than the G3 value, indicating that the G3 barrier is somewhat thinner.

3. Computational details

Home-made QCT procedure was used for trajectory calculation. The computational details have been described by Karplus, Porter, and Sharma [27]. In our previous work [28,29], we found the Runge–Kutta method provided poor conservation of energy. In order to maintain the conservational property in numerical solution of Hamiltonian systems, we applied symplectic integration method [30–32] in the QCT study. The step size used in all calculations reported here was 1.08×10^{-16} s.

The calculations on the new mBW2 PES have been performed for the $Cl + HD$ (v, j) reaction at collision energies, $E_c = 0.2775$ eV, 0.65 eV, for $v = 0$, 1, 2, $j = 0$, 1, 3, 5, 10, and total energy, $E_{tot} = 1.5$ eV, for $v = 0$, 1, 2, $j = 0$, 2, 4. Batches of 10 000 trajectories were run for every set of v, j, E_c or E_{tot}, respectively.

The final state properties obtained for each trajectory were the identity of the molecular product, the translational and internal energies, and the scattering angle θ. The internal energy of the product molecule was partitioned into vibrational and rotational contributions. The continuous classical values of the vibrational and rotational states, v' and j', respectively, corresponding to these energies, were rounded off to the nearest integer.

4. Results and discussion

4.1. Reaction cross-sections

The reaction cross-sections $S_r(v, j, E_c)$ for a set of initial conditions were calculated from the equations:

$$S_r(v, j, E_c) = \pi b_{max}^2(E_c)[N_r(v, j, E_c)/N(v, j, E_c)], \quad (7)$$

where $N_r(v, j, E_c)$ and $N(v, j, E_c)$ are the number of reactive collisions and the number of total collisions, respectively. The $b_{max}(E_c)$ is the maximum impact parameter.

Table 2 lists the reaction cross-sections, S_r (DCl) and S_r (HCl), and the isotopic branching ratio, defined as $\Gamma = S_r$ (DCl)/S_r (HCl), at collision energy $E_c = 0.2775$ eV. It shows that S_r (DCl) and S_r (HCl) increase considerably with increasing v at a

Table 2
Reaction cross-section S_r (v, j, $E_c = 0.2775$ eV) for Cl + HD reaction

v	j	E_{tot} (eV)	S_r (DCl) (a_0^2)	S_r (HCl) (a_0^2)	Γ (DCl/HCl)
0	0	0.51	0.053	0.021	2.52
	1	0.52	0.48	0.055	8.73
	3	0.58	1.44	1.53	0.94
	5	0.68	0.46	1.87	0.24
	10	1.14	4.20	12.6	0.33
1	0	0.97	11.9	1.36	8.75
	1	0.98	15.4	3.30	4.67
	3	1.04	11.8	10.8	1.09
	5	1.14	14.9	9.76	1.53
	10	1.6	16.3	17.6	0.93
2	0	1.4	24.6	7.00	3.51
	1	1.41	22.6	9.20	2.46
	3	1.47	21.8	15.7	1.39
	5	1.57	19.1	16.8	1.14
	10	2.02	19.3	25.9	0.74

given j. At a given j, Γ (DCl/HCl) is the maximum at $v = 1$ except $j = 1$, where Γ (DCl/HCl) is the maximum at $v = 0$. At a given v, S_r (HCl) in general increases with increasing j. At $v = 0$, 1, S_r (DCl) in general increases with increasing j, whereas, at $v = 2$, S_r (DCl) in general decreases with increasing j except $j = 10$. In addition, at $E_c = 0.2775$ eV, $v = 1$, $j = 1$, Γ (DCl/HCl) is 4.67, whereas this Γ (DCl/HCl) on the G3 PES is 1.34 [16]. At the other initial condition, the Γ (DCl/HCl) on the mBW2 PES is also larger than that on the G3 PES. Moreover, the experimental value [17] of Γ (DCl/HCl) ($v = 1$, $j = 1$) is three times larger than the theoretical value on the G3 PES at the mean collision energy of 0.065 eV. Therefore the results on the mBW2 PES are better than that on the G3 PES compared with the experiment [17].

Comparing S_r ($v = 0$, $j = 10$, $E_c = 0.2775$ eV) with S_r ($v = 1$, $j = 5$, $E_c = 0.2775$ eV), it is found that the total energy E_{tot} is the same. S_r (DCl; $v = 0$, $j = 10$, $E_c = 0.2775$ eV), 4.20 a_0^2, is smaller than S_r (DCl; $v = 1$, $j = 5$, $E_c = 0.2775$ eV), 14.9 a_0^2, whereas S_r (HCl; $v = 0$, $j = 10$, $E_c = 0.2775$ eV), 12.6 a_0^2, is larger than S_r (HCl; $v = 1$, $j = 5$, $E_c = 0.2775$ eV), 9.76 a_0^2. It means that the vibrational energy is more effective than the rotational energy for the DCl isotopic reaction channel, whereas the rotational energy is more effective than the vibrational energy for the HCl isotopic reaction channel. At $E_c = 0.65$ eV, the phenomena are similar. S_r (DCl; $v = 0$, $j = 10$, $E_c = 0.65$ eV), 14.2 a_0^2, is also smaller than S_r (DCl; $v = 1$, $j = 5$, $E_c = 0.65$ eV), 18.4 a_0^2; S_r (HCl; $v = 0$, $j = 10$, $E_c = 0.65$ eV), 14.8 a_0^2, is also larger than S_r (HCl; $v = 1$, $j = 5$, $E_c = 0.65$ eV), 13.7 a_0^2.

Table 3
Reaction cross-section S_r (v, j, E_c) at $E_{tot} = 1.5$ eV for Cl + HD reaction

v	j	E_c (eV)	S_r (DCl) (a_0^2)	S_r (HCl) (a_0^2)	Γ (DCl/HCl)
0	0	1.26	17.3	4.00	4.32
	2	1.23	16.4	5.10	3.21
	4	1.15	17.0	6.19	2.75
1	0	0.81	22.3	7.53	2.96
	2	0.77	22.7	8.59	2.64
	4	0.69	21.5	12.8	1.68
2	0	0.38	25.0	8.48	2.95
	2	0.34	24.9	13.4	1.86
	4	0.26	19.1	19.8	0.96

In order to compare the effectiveness of the translational energy with that of the rotational energy and that of vibrational energy, S_r and Γ (DCl/HCl) at the total energy $E_{tot} = 1.5$ eV are listed in Table 3. At a given v, S_r (HCl) increases with increasing j, and Γ (DCl/HCl) decreases with increasing j. It means that the rotational energy is more effective than the translational energy for the HCl isotopic reaction channel. At a given j, S_r (DCl) and S_r (HCl) increase with increasing v except S_r (DCl) at $v = 2$, $j = 4$, and Γ (DCl/HCl) decreases with increasing v. Vibrational energy is more effective than the translational energy for both isotopic reaction channels. In summary, for the HCl isotopic reaction channel, the rotational energy is most effective, and that of the translational energy is least; for the DCl isotopic reaction channel, the vibrational energy is most effective.

4.2. Product energy partitioning and angular distribution

Table 4 lists the average vibrational, rotational, translational energies, $\langle E'_v \rangle$, $\langle E'_R \rangle$, $\langle E'_{tr} \rangle$, respec-

Table 4
Average product energies at collision energy $E_c = 0.2775$ eV

v	j	Cl + DH → DCl + H			Cl + HD → HCl + D		
		$\langle E'_v \rangle$	$\langle E'_R \rangle$	$\langle E'_{tr} \rangle$	$\langle E'_v \rangle$	$\langle E'_R \rangle$	$\langle E'_{tr} \rangle$
0	0	0.20	0.02	0.29	0.20	0.07	0.24
	1	0.19	0.04	0.29	0.24	0.04	0.24
	3	0.21	0.04	0.33	0.21	0.07	0.30
	5	0.15	0.07	0.46	0.20	0.11	0.37
	10	0.17	0.23	0.74	0.22	0.27	0.65
1	0	0.26	0.13	0.58	0.31	0.14	0.52
	1	0.29	0.11	0.58	0.25	0.18	0.55
	3	0.3	0.13	0.61	0.27	0.20	0.57
	5	0.24	0.20	0.70	0.28	0.22	0.64
	10	0.22	0.34	1.04	0.28	0.38	0.94
2	0	0.40	0.21	0.79	0.37	0.27	0.76
	1	0.46	0.15	0.80	0.38	0.26	0.77
	3	0.37	0.25	0.85	0.35	0.31	0.81
	5	0.45	0.23	0.89	0.40	0.34	0.83
	10	0.38	0.35	1.29	0.41	0.48	1.13

Table 5
Average scattering angles $\langle \theta \rangle$

v	j	$E_c = 0.2775$ eV		$E_c = 0.65$ eV	
		Cl + DH	Cl + HD	Cl + DH	Cl + HD
0	0	123	145	107	107
	1	119	141	109	110
	3	114	134	110	116
	5	111	116	107	111
	10	78	111	87	102
1	0	93	113	100	100
	1	100	115	99	102
	3	95	113	101	103
	5	91	104	99	102
	10	93	88	95	92
2	0	94	104	104	96
	1	94	102	98	92
	3	95	104	99	95
	5	85	90	96	92
	10	80	89	91	81

tively, of the products (DCl and HCl), for each initial state v, j at collision energy $E_c = 0.2775$ eV. It is found that $\langle E'_{tr} \rangle$ of DCl is larger than $\langle E'_{tr} \rangle$ of HCl for the same initial state, whereas $\langle E'_R \rangle$ of DCl is smaller than $\langle E'_R \rangle$ of HCl for the same initial state. For the two isotopic reaction channels, all of $\langle E'_v \rangle$, $\langle E'_R \rangle$ and $\langle E'_{tr} \rangle$ increase with increasing v at a given j, but $\langle E'_{tr} \rangle$ has a main increase; $\langle E'_R \rangle$ has only a minor increase. At a given v, $\langle E'_{tr} \rangle$ mainly increases with increasing j; $\langle E'_R \rangle$ in general increases with increasing j. It means that the rotational energy of reagents hardly appears as product vibrational energy.

Average scattering angles $\langle \theta \rangle$ of the products are listed in Table 5. At the collision energy $E_c = 0.2775$ eV, the average scattering angle $\langle \theta \rangle$ is larger for the product HCl than for DCl. For the two isotopic reaction channels, $\langle \theta \rangle$ in general decreases with increasing j at a given v; it also decreases with increasing v at a given j. However, at the collision energy $E_c = 0.65$ eV, the phenomena are different. $\langle \theta \rangle$ of HCl channel is almost the same as that of DCl channel. $\langle \theta \rangle$ is not dependent to any significant extent on j or v. This is reasonable, because the scattering angle mainly depends on the translational energy at high collision energy.

The product angular distributions at some given initial conditions are shown in Fig. 1. At $E_c =$ 0.2775 eV, the percent of forward scattering and sideways scattering for the DCl channel is larger than that for the HCl channel. For both reaction channels, this percent increases when j or v turns from zero to one at $E_c = 0.2775$ eV; it also increases when the collision energy turns from 0.2775–0.65 eV at $j = 0$, $v = 0$.

4.3. Product rotational and vibrational state distribution

The product rotational distributions at some given initial conditions are shown in Fig. 2. The rotational distribution is broad except for the DCl channel at $E_c = 0.2775$ eV, $v = 0$, $j = 0$. At high collision energy $E_c = 0.65$ eV, the percent of high rotationally excited states obviously increases compared with that at $E_c = 0.2775$ eV. This percent also increases with increasing initial vibrational state v.

The product vibrational distributions at some given initial conditions are shown in Fig. 3. For both isotopic reaction channels, the product vibrational state (v') is mainly at the ground state under the conditions of our calculations; the product vibrational state is hardly excited. The percent of the vibrationally excited states will slightly increase when initial internal state v, j or the collision

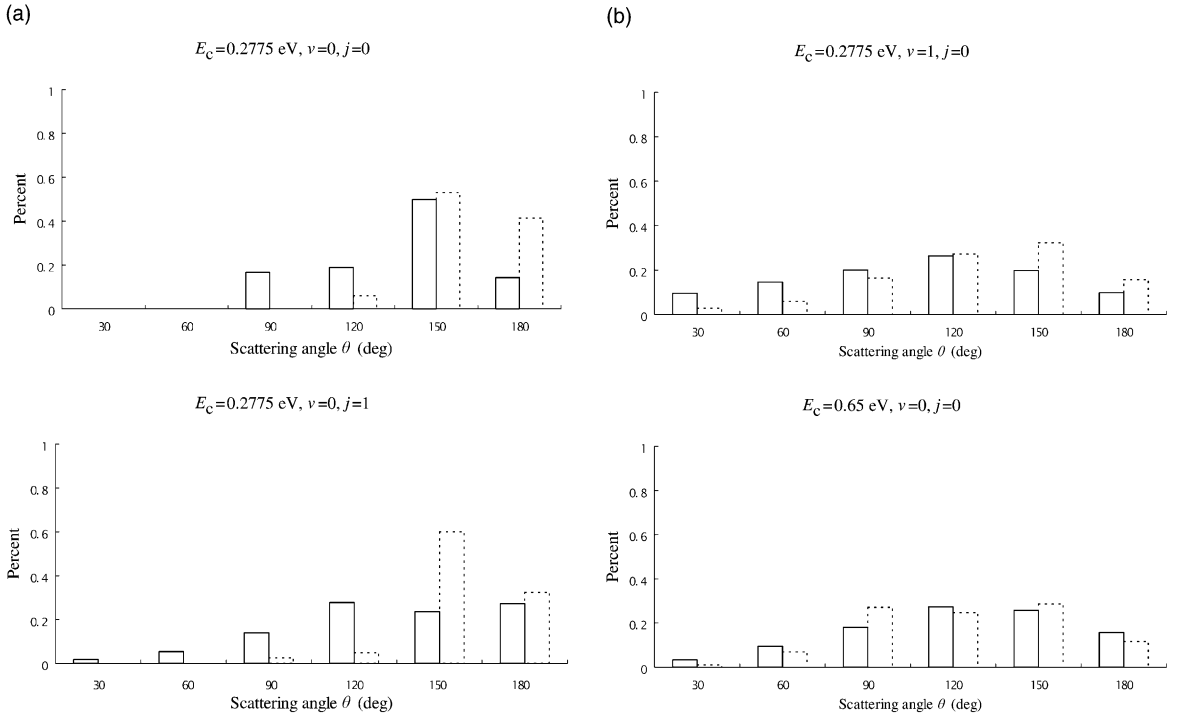

Fig. 1. Product angular distribution. (—): Cl + DH → DCl + H; (- - -): Cl + HD → HCl + D.

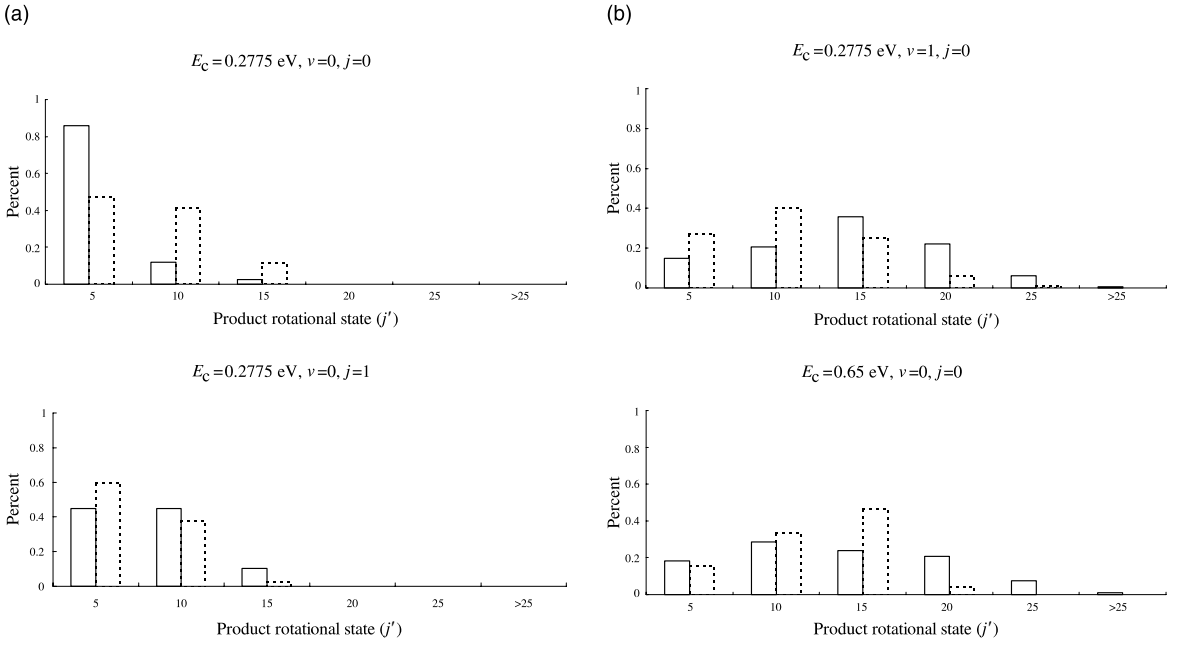

Fig. 2. Product rotational state distribution. (—): Cl + DH → DCl + H; (- - -): Cl + HD → HCl + D.

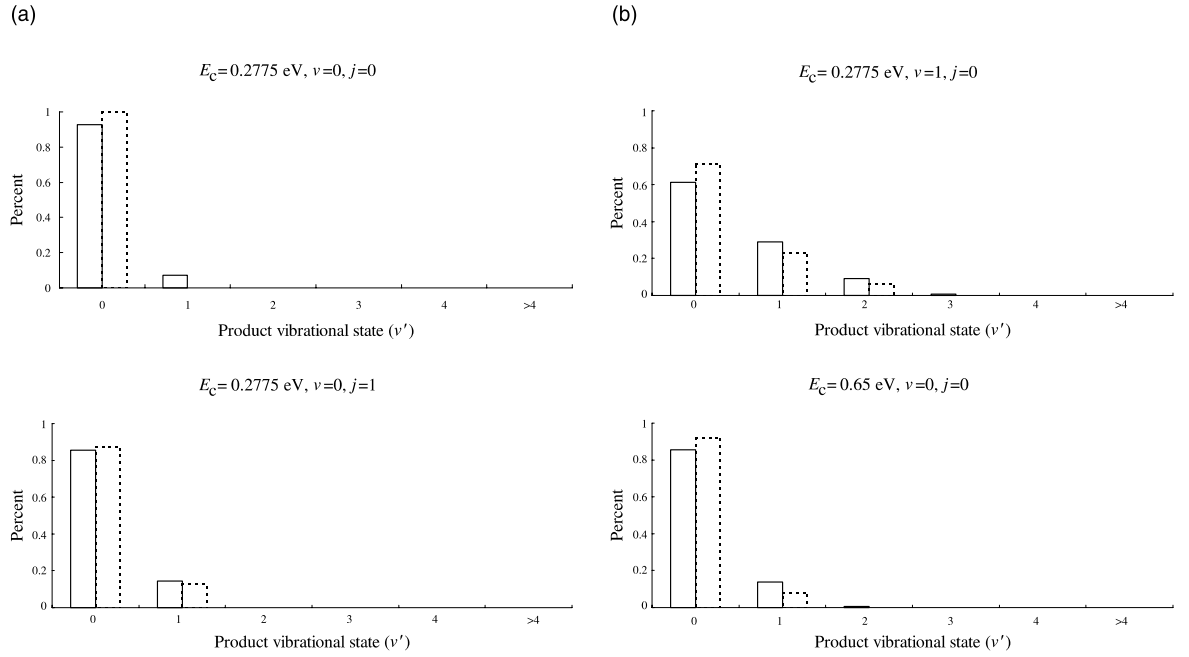

Fig. 3. Product vibrational state distribution. (—): Cl + DH → DCl + H; (- - -): Cl + HD → HCl + D.

energy E_c increases. However, this percent is always a little larger for the DCl channel than for the HCl channel at a given initial condition. On the G3 PES, the HCl channel shows a considerable degree of vibrational adiabaticity; the vibrational distribution of the DCl channel is broader than that of the HCl channel. Maybe because the mBW2 surface has a well in the exit channel, which the G3 surface has not, the product internal state distribution on the two surfaces is different. The mBW2 surface is anisotropic in the exit channel because of the well. Moreover, the rotational energy level of the products is small; the vibrational energy level of the products is large. Therefore, the product rotational state is easily excited, whereas the product vibrational state is hardly excited.

5. Conclusions

In a summary, the following conclusions can be obtained for the Cl + HD reaction on the mBW2 PES from QCT calculation.

(1) The Γ (DCl/HCl) on the mBW2 PES is also larger than that on the G3 PES at the same initial condition. The calculational results on the mBW2 PES are better than that on the G3 PES when compared with the experiment [17].

(2) For the HCl isotopic reaction channel, the rotational energy is most effective, and that of the translational energy is least. However, for the DCl isotopic reaction channel, the vibrational energy is most effective.

(3) The rotational energy of reagents is not easily converted into the vibrational energy of the products. The other energies can interconvert more readily.

(4) The average scattering angle $\langle\theta\rangle$ of the products in general decreases with increasing v or j at the collision energy $E_c = 0.2775$ eV. However, at the collision energy $E_c = 0.65$ eV, $\langle\theta\rangle$ changes only slightly when v or j increases.

(5) The product rotational state is easily excited, and the product rotational distribution is broad. However, the product vibrational state is hardly excited.

Acknowledgement

This work was supported by National Natural Science Foundation of China.

References

[1] J.C. Miller, R.T. Gordon, J. Chem. Phys. 78 (1983) 3713.
[2] S.C. Tucker, D.G. Truhlar, B.C. Garrett, A.D. Isaacson, J. Chem. Phys. 82 (1985) 4102.
[3] D.W. Schwenke, S.C. Tucker, R. Steckler, F.B. Brown, G.C. Lynch, D.G. Truhlar, B.C. Garrett, J. Chem. Phys. 90 (1989) 3110.
[4] G. Ju, W. Bian, E.R. Davison, Theor. Chim. Acta 83 (1992) 331.
[5] W. Bian, G. Ju, Chem. J. Chin. Univ. 14 (1993) 857.
[6] M. Alagia, N. Balucani, P. Casavecchia, D. Stranges, G.G. Volpi, J. Chem. Soc., Faraday Trans. 91 (1995) 575.
[7] M. Alagia, N. Balucani, L. Cartechini, P. Casavecchia, E.H. Van Kleef, G.G. Vopli, F.J. Aoiz, L. Bañares, D.W. Schwenke, T. Allison, S.L. Mielke, D.G. Truhlar, Science 273 (1996) 1519.
[8] T.C. Allison, G.C. Lynch, D.G. Truhlar, M.S. Gordon, J. Phys. Chem. 100 (1996) 13575.
[9] S.-H. Lee, L.H. Lai, K. Liu, J. Chem. Phys. 110 (1999) 8229.
[10] D. Skouteris, D.E. Manolopoulos, W. Bian, H.-J. Werner, L.H. Lai, K. Liu, Science 286 (1999) 1713.
[11] M.J. Stern, A. Persky, F.S. Klein, J. Chem. Phys. 58 (1973) 5697.
[12] A. Persky, J. Chem. Phys. 66 (1977) 2932.
[13] A. Persky, J. Chem. Phys. 68 (1978) 2411.
[14] A. Persky, J. Chem. Phys. 70 (1979) 3910.
[15] A. Persky, M. Broida, J. Chem. Phys. 84 (1986) 2653.
[16] F.J. Aoiz, L. Bañares, Chem. Phys. Lett. 247 (1995) 232.
[17] S.A. Kandal, A.J. Alexander, Z.H. Kim, R.N. Zare, F.J. Aoiz, L. Bañares, J.F. Castillo, V.S. Rábanos, J. Chem. Phys. 112 (2000) 670.
[18] W. Bian, H.-J. Werner, J. Chem. Phys. 112 (2000) 220.
[19] U. Manthe, W. Bian, H.-J. Werner, Chem. Phys. Lett. 313 (1999) 647.
[20] B. Yang, H. Gao, K. Han, J.Z.H. Zhang, J. Chem. Phys. 113 (2000) 1434.
[21] B. Yang, H. Gao, K. Han, J.Z.H. Zhang, J. Chem. Phys. 113 (2000) 7182.
[22] H.-J. Werner, P.J. Knowles, J. Chem. Phys. 89 (1988) 5803.
[23] H.-J. Werner, P.J. Knowles, J. Chem. Phys. 82 (1985) 5053.
[24] S.R. Langhoff, E.R. Davidson, Int. J. Quant. Chem. 8 (1974) 61.
[25] R. Steckler, D.W. Schwenke, F.B. Brown, D.G. Truhlar, Chem. Phys. Lett. 121 (1985) 475.
[26] http://thechem.edu.chinaren.com.
[27] M. Karplus, R.N. Porter, R.D. Sharma, J. Chem. Phys. 43 (1965) 3259.
[28] G. Ju, D. Feng, C. Deng, Theor. Chim. Acta 74 (1988) 403.
[29] G. Ju, D. Feng, C. Deng, Scientica Sinica (B) 9 (1987) 920.
[30] K. Feng, H. Wu, M. Qin, D. Wang, J. Comp. Math. 7 (1989) 71.
[31] H. Yoshida, Phys. Lett. A 150 (1990) 262.
[32] Ch. Schlier, A. Seiter, J. Phys. Chem. A 102 (1998) 9939.